Noise-NeRF: Hide Information in Neural Radiance Fields using Trainable Noise

Qinglong Huang, Yong Liao, Yanbin Hao, Pengyuan Zhou*

University of Science and Technology of China

qinglonghuang@mail.ustc.edu.cn, yliao@ustc.edu.cn, haoyanbin@hotmail.com, zpymyyn@gmail.com

Abstract—Neural radiance fields (NeRF) have been proposed as an innovative 3D representation method. While attracting lots of attention, NeRF faces critical issues such as information confidentiality and security. Steganography is a technique used to embed information in another object as a means of protecting information security. Currently, there are few related studies on NeRF steganography, facing challenges in low steganography quality, model weight damage, and a limited amount of steganographic information. This paper proposes a novel NeRF steganography method based on trainable noise: Noise-NeRF. Furthermore, we propose the Adaptive Pixel Selection strategy and Pixel Perturbation strategy to improve the steganography quality and efficiency. The extensive experiments on open-source datasets show that Noise-NeRF provides state-of-the-art performances in both steganography quality and rendering quality, as well as effectiveness in super-resolution image steganography.

Index Terms—neural radiation fields, steganography, implicit neural representation

I. INTRODUCTION

The neural radiance fields (NeRF) have been rapidly evolving and made breakthroughs in its application to 3D reconstruction [1]. NeRF can reconstruct three-dimensional photorealistic scenes from limited 2D image data from different viewpoints while ensuring scene continuity [2]. NeRF holds great potential in digital media such as virtual reality, augmented reality, special effects games, etc [3].

Meanwhile, the information confidentiality and data security issues of NeRF have become increasingly important concerns [4], yet with very few studies so far. This article focuses on NeRF steganography, aiming to embed secret information into NeRF while hiding its existence and accurately recover the steganographic hidden information. This is of great significance for research on embedding information into trained NeRF models through steganography to protect the confidentiality of the information or the copyright of the model.

NeRF steganography has been proposed recently [5], [6]. The current approach, which embeds and recovers hidden information into and from the NeRF model through retraining, has several shortcomings. First, current methods inevitably damage the model due to their approach of embedding secret information into the model weights. Consequently, they commonly present different reconstruction qualities under different viewing angles [6]. Secondly, they lack effectiveness in terms of the amount of steganographic information. Current methods mainly embed information in a single image or binary code
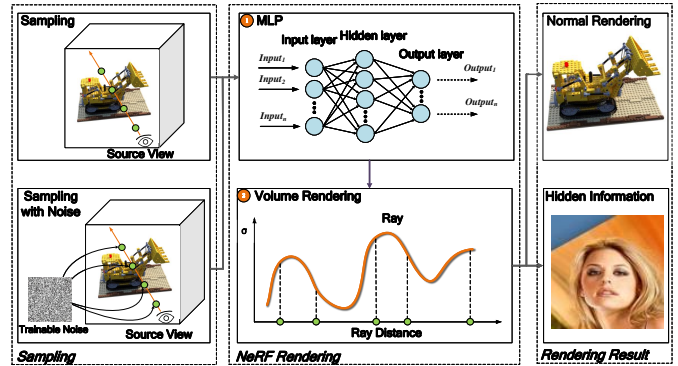

Fig. 1: Overview of Noise-NeRF.

for a single NeRF scene, which would face quality collapse if embedding too much information. Finally, current methods mainly work with low-quality images while hiding information in super-resolution images is still overlooked.

To deal with the mentioned challenges, this paper proposes a novel NeRF steganography method based on trainable noise: Noise-NeRF (see Fig. 1). Noise-NeRF takes advantage of the neural networks in NeRF to query color and density information. We introduce trainable noise on specific views to achieve information steganography. The NeRF model renders the hidden information when we input the noise into the NeRF model during sampling, otherwise renders the normal images. Our method only needs to update the input noise, without embedding a backdoor through the process of NeRF training. In other words, our method doesn't change the weights of the NeRF model, thus maintaining the rendering quality with no loss. Moreover, the amount of hidden information only depends on the noise in our method. That is, by inputting different noises into the model, different hidden information can be rendered. Noise-NeRF can achieve an unlimited amount of steganographic information for a single NeRF scene, which improves the steganographic capability of the model without damaging the steganographic quality. The contribution of this article can be summarized as follows:

- We studied the problems of NeRF steganography and proposed the first lossless NeRF steganography method: Noise-NeRF, by updating the input noise at a specific view rather than the model's weights. Our method ensures the NeRF model achieves information steganography

without impacting its rendering quality.

- We propose an Adaptive Pixel Selection Strategy and a Pixel Perturbation Strategy to select pixels with greater differences according to the gradient to update the noise. We update the input noise in the early stage and finely process the pixel details of hidden content in the later stage. Our strategies significantly improve the recovery quality and steganography efficiency of NeRF steganographic information.
- We conduct extensive experiments on ImageNet and several famous super-resolution image datasets using a series of pre-trained NeRF scenes. The experiments show that our method reaches the SOTA level in both steganography quality and rendering quality in NeRF.

II. RELATED WORK

A. Neural Radiance Fields

The success of NeRF [7] has drawn widespread attention to the simple and high-fidelity three-dimensional reconstruction method of neural implicit representation. Implicit representation is a continuous representation that can be used for the generation of new perspectives and usually does not require 3D signals for supervision. NeRF realizes an effective combination of neural fields and graphics component Volume rendering [7]. It uses a neural network to implicitly simulate the scene. By inputting the spatial coordinates of the three-dimensional object, NeRF outputs the corresponding geometric information. There are currently many improvements and application research on NeRF, including accelerated training of NeRF [8]–[10], editing research on NeRF [11]–[13], generalization research on NeRF [14]–[17], and large-scale scenes [18], [19], etc. These studies have made NeRF's three-dimensional reconstruction efficient and have practical applications in many scenes. With the launch of NeRF-related products such as Luma AI [20], issues such as information security and copyright protection for NeRF have become increasingly important.

B. Steganography for 2D Image

Steganography for 2D images is an important direction in the field of information security, which uses 2D images as a carrier. Traditional image steganography methods generally use redundant information in the image to hide secret information [21]. For example, the most popular technique is "least significant bit" (LSB) steganography [22]–[24]. The idea of this method is to embed secret information into the least significant bits of the pixel values of 2D images. The LSB algorithm can hide a large amount of content, make small changes to the image, and is difficult to detect. With the development of deep neural networks, there are also many studies using neural networks for information hiding [25]–[27]. DeepStega [27] can hide the steganographic image in a carrier of the same size. As the representation model of 3D scenes based on neural radiation fields has received widespread attention, steganography for NeRF will become an important research direction.

C. Steganography to NeRF

In the past, explicit representation was generally used to represent 3D scenes, such as Mesh, Point Cloud, Voxel, and Volume [28]. These representations enable explicit modeling of scenes. They are also convenient for extending the steganography method of 2D images to 3D scenes, such as [29]–[31]. However, the NeRF method for implicit representation is completely different. It maps the coordinate information of each point in the spatial scene to the color and density of the point. The internal weights make it difficult to accurately express the physical meaning with clear interpretability. Therefore, explicit translation, rotation, scaling, embedding, and other steganographic measures are difficult to use on NeRF.

In response to the difficulties of NeRF steganography, in 2022, StegaNeRF [6] studied information hiding in NeRF for the first time. They hide natural images into 3D scene representations by retraining NeRF parameters, and simultaneously train a decoder that can accurately extract hidden information from NeRF-rendered 2D images. In 2023, CopyRNeRF [5] studied copyright protection research for NeRF. They protect the copyright of the NeRF model by replacing the original color representation in NeRF with the color representation of watermarks. They use a decoder to recover the binary secret information from the rendered image while maintaining high rendering quality and allowing watermark extraction. Although effectively performing NeRF steganography, their method faces issues such as model retraining, hiding volume, and steganography quality.

III. METHOD

As discussed in Section I, directly embedding the hidden information in the NeRF model would change the model weights and thus limit the quality of steganography. In contrast to previous NeRF steganography methods, Noise-NeRF adopts a completely new approach. Instead of modifying the model weights, Noise-NeRF determines the steganographic information on the input trainable noise, which is optimized iteratively.

A. NeRF Preliminary

NeRF reconstruction method [7] models three-dimensional scenes from two-dimensional pictures. NeRF represents a continuous scene in space as a 5D neural radiation fields. NeRF inputs the position information (x, y, z) and direction information (ψ, ϕ) of a specific point in the scene and outputs color information c and voxel density information $sigma$. The neural radiation fields F_θ with trainable parameters θ can be expressed as:

$$F_\theta : (x, y, z, \psi, \phi) \rightarrow (c, \sigma) \tag{1}$$

Next, NeRF uses the volume rendering formula to sample the rays along the observation direction and passes the sampled 3D points through the neural network to obtain the pixel value c and voxel density σ of each point for sampling and

superposition to finally obtain the pixel value corresponding to this ray direction:

$$C(\mathbf{r}) = \int_{t_n}^{t_f} T(t)\sigma(\mathbf{r}(t))\mathbf{c}(\mathbf{r}(t), \mathbf{d})dt$$
$$\text{where } T(t) = \exp\left(-\int_{t_n}^{t} \sigma(\mathbf{r}(s))ds\right) \quad (2)$$

where $C(r)$ denotes the color rendered by the camera ray $r(t) = o + td$, t_n denotes the near boundary, t_f denotes the far boundary, and $T(t)$ represents the cumulative transmittance along the ray from t_n to t.

NeRF also adopts a hierarchical sampling strategy to train and optimize the network parameters θ through the mean square error (MSE loss) between the rendered and the true pixel colors. This enables NeRF to learn implicit representations and capture the features of 3D scenes, as expressed in Eq.(3).

$$L = \sum_{r \in R} \left[\left\| \hat{C}_c(r) - C_{GT}(r) \right\|_2^2 + \left\| \hat{C}_f(r) - C_{GT}(r) \right\|_2^2 \right] \quad (3)$$

where R represents all the rays in the input viewpoint, $C_c(r)$ and $C_f(r)$ represent the color prediction of the ray by the coarse network and the fine network, respectively. $C_{GT}(r)$ denotes the ground truth.

B. Noise Optimization

The goal of Noise-NeRF is to embed the steganographic information into the noise by calculating the gradient and updatting the noise. Let θ denote the weight of a pre-trained NeRF scene and M denote the hidden information. For a certain viewpoint P, a normal picture C can be obtained through NeRF rendering, that is, $f_\theta(P) = C$. We aim to generate noise δ through Noise-NeRF so that the model can render the steganographic content M, that is, $f_\theta(P + \delta) = M$.

The implementation framework of Noise-NeRF is shown in Fig. 2. Noise-NeRF is inspired by adversarial attack [32], which is a method that makes small perturbations to the original input samples to cause the neural network to produce misclassification or wrong output [33]. We add noise under a specific viewpoint to cause the NeRF's neural network to produce intentional error output, thus NeRF can render the hidden information. Since adversarial attack examples commonly show better results in high-dimensional space [34], and NeRF maps low-dimensional coordinate points and directions to high-dimensional space through positional encoding [7] (Eq. (4)) to improve the network's ability to capture high-frequency information [35], we add noise after positional encoding in Noise-NeRF.

$$\gamma(p) = \left(\sin\left(2^0 \pi p\right), \cos\left(2^0 \pi p\right), \cdots, \cos\left(2^{L-1} \pi p\right)\right) \quad (4)$$

We add noise to the 5D coordinate points after positional encoding and then perform three-dimensional rendering through NeRF's MLP. The goal is to minimize the difference between the steganographic image and the image generated by the original NeRF by calculating the following loss.

$$L_{rgb} = \sum_{r \in R} \sum_{p \in r} \left[\left\| \hat{C}_f(\gamma(p) + \delta) - C_M(\gamma(p)) \right\|_2^2 \right] \quad (5)$$

where R represents all the rays in the input viewpoint, r represents one of the rays, δ is the added noise, C_M is the steganographic target information.

Noise-NeRF calculates the gradient of the model via backpropagation to find the best direction to perturb the input sample. We then update the input noise along the direction of the gradient so that the NeRF model can produce steganographic information, as follows.

$$\delta_p^i = \delta_p^{i-1} + \eta \cdot Adam(\nabla_{\delta_p^t} \widetilde{L}_{rgb}) \quad (6)$$

where δ_p^t represents the noise added to the p sampling point in the i iteration process, and η is the learning rate.

In summary, by iteratively training noise on a specific viewpoint, the NeRF model can produce error rendering results as shown in Fig. 3(a) and (c). However, if noise is added to other viewpoints (subfig(c) and (d)), the steganographic image cannot be rendered, and the rendered image has a large residual difference from the ground truth. This makes Noise-NeRF steganography highly concealed and difficult to be detected.

C. Adaptive Pixel Selection

Though we calculate the gradient information of the input noise and update it through backpropagation, not all pixels are equally sensitive to the input noise. Different pixels between the steganographic target and NeRF's predicted image would cause different loss values and require different iteration settings to generate better noise. Therefore, we refer to the idea of batch size adaptation [36] and propose Adaptive Pixel Selection strategy, which adaptively selects pixels and sets different iterations.

Given a set of pixel batch sizes $S = s_1, ..., s_m$, we select each batch size s_i ($\forall s_i \in S$) in one iteration, compute the gradient, and update the input noise. To measure the impact of different batch sizes on steganography performance, we assume that the convergence speed remains stable within an iteration. If the batch size $s_i(s_i \in S)$ reduces the average loss the most in each query, it is considered the most appropriate batch size. Our method shares the gradients computed in the maximum batch size.

D. Pixel Perturbation Strategy

When updating noise, we aim to recover the steganographic information M from the camera pose P of the selected viewpoint. For the relatively NeRF network, using iterative loss calculation (Eq. (5)) and backpropagation is computationally heavy. Therefore, we target a fast deviation of the rendered image from the original image in the early stage of the noise update process. To achieve that, we need the noise to cause false positives in rendering $f_\theta(P + \delta)$ as much as possible.
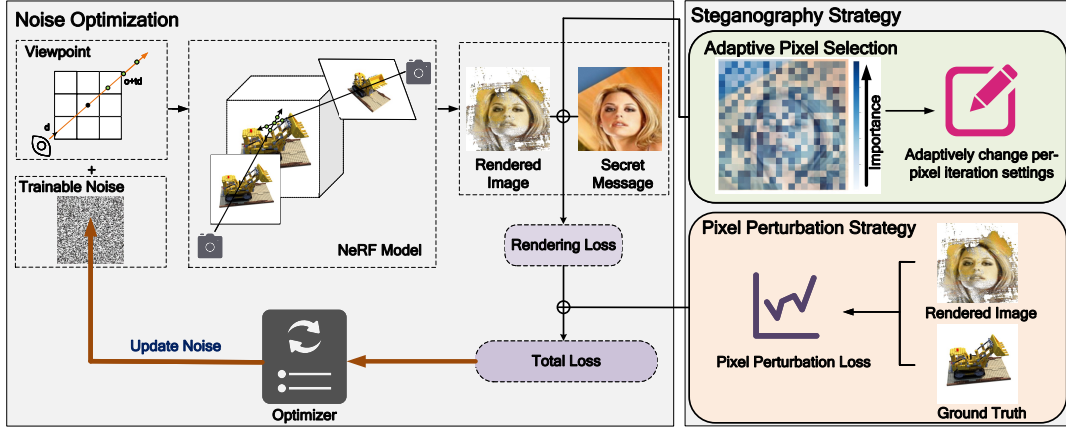
Fig. 2: Framework of Noise-NeRF.

(a) Noise to Certain Viewpoint (b) Noise to Other Viewpoint

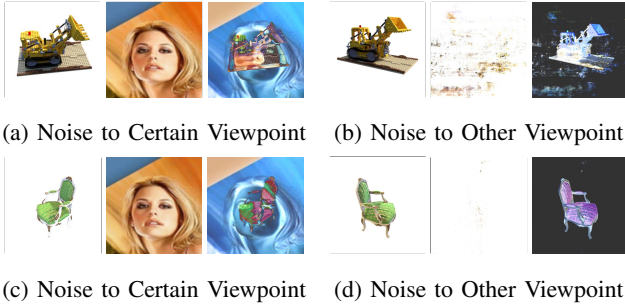(c) Noise to Certain Viewpoint (d) Noise to Other Viewpoint

Fig. 3: Results of applying Noise-NeRF on scenes of Lego (top) and Chair (bottom). (a) and (c) depict the rendering results for a specific view. (b) and (d) depict the rendering results for other views. In each subfigure, from left to right are the rendered image without noise input, with noise input, and the residuals of the rendered image and Ground Truth.

Therefore, we refer to the idea of batch size adaptation [36] and propose the Pixel Perturbation Strategy as follows.

$$L_{perturb} = - \sum_{r \in R} \sum_{p \in r} \left[\left\| \hat{C}_f(\gamma(p) + \delta) - \hat{C}_f(\gamma(p)) \right\|_2^2 \right] \quad (7)$$

As such, we increase the efficiency of steganography by combining the fast deviation of the image in the early image thanks to the Pixel Perturbation Strategy, and, optimization of the rendered image thanks to the Adaptive Pixel Selection. The overall training loss of Noise-NeRF is expressed as:

$$\begin{cases} L = \lambda_1 \cdot L_{rgb} + \lambda_2 \cdot L_{perturb}, \ iteration \leq \mu \\ L = L_{rgb}, \ iteration > \mu \end{cases} \quad (8)$$

where λ_1 and λ_2 are coefficients that control the weight of the two loss functions, and μ is the boundary value of iteration.

To sum up, the input noise will be updated through back-propagation by calculating its loss gradient. This can generate the noise that causes the neural network to output incorrectly, and achieve lossless steganography in NeRF. Further, we propose Adaptive Pixel Selection and Pixel Perturbation Strategy to significantly improve the quality and efficiency of NeRF steganography. The overall process of the Noise-NeRF is summarized in Algorithm 1.

Algorithm 1 Noise-NeRF on a single scene

Input: Pretrained NeRF model f and weights θ, Secret Message M, Viewpoint P
Output: Well-trained noise δ
for each iteration t **do**
    Conduct Adaptive Pixel Selection
    Add noise to NeRF rendering $f_\theta(P + \delta_p)$
    Compute rgb loss L_{rgb} in Eq. (5)
    Compute Perturbation loss $L_{perturb}$ in Eq. (7)
    Compute total loss L in Eq. (8)
    Update Noise $\delta^i = \delta^{i-1} + \eta \cdot Adam(\nabla_{\delta^t} L)$
end for

IV. EXPERIMENTS

A. Environment Settings

Datasets and hyperparameter settings. We chose the standard NeRF as the experimental object. For forward and 360° scenes, we selected scenes in LLFF [37] and NeRF-Synthetic [7] as objects respectively. We randomly selected images from imagenet [38] as steganographic targets. We also selected some popular super-resolution datasets: DIV2K [39], OST [40], FFHQ [41], CeleA-HQ [42] to test the super-resolution steganography performance of Noise-NeRF. The hyperparameters in Eq.(8) are set as $\gamma_1 = 0.5$, $\gamma_2 = 0.5$, and $\mu = 50$. The learning rate of each iteration is set to 1e-2, and the learning decay rate is set to 0.3. All the experiments were conducted on a server equipped with an NVIDIA RTX3090 GPU and 16GB of memory.

Metrics. We use PSNR, SSIM, and LPIPS, the classic indicators for measuring 3D reconstruction quality in NeRF, to

evaluate the NeRF rendering effect. We use SSIM and SNR to evaluate the recovery quality of steganographic information. **Baselines.** For the current SOTA method StegaNeRF [6], we use its original settings; for the traditional algorithm LSB [43] for two-dimensional pictures and the deep learning algorithm DeepStega [26], we hide the information in the two-dimensional images of the training dataset, and then use the traditional NeRF training method.

B. Multiple Scenes Steganography

We select specified viewpoints for NeRF steganography on different scenes and use Noise-NeRF to generate noise. Then we input the noise into the NeRF model to render a steganographic image to verify the quality of NeRF steganography. In addition, we also verify the impact of each baseline on NeRF rendering quality. The qualitative and quantitative results are shown in Fig. 4 and Table. I.

TABLE I: Performance comparisons on multiple scenes. Standard NeRF is an initial NeRF scenario trained with standard settings. The upper part of the table is tested on the NeRF-Synthetic dataset; the lower part is tested on the LLFF dataset. The results are the average values across different scenes.

Method	NeRF Rendering			Embed Recovery	
	PSNR	SSIM	LPIPS	SSIM	ACC(%)
Standard NeRF [7]	27.74	0.8353	0.1408	N/A	N/A
LSB [24]	27.72	0.8346	0.1420	0.0132	N/A
DeepStega [27]	26.55	0.8213	0.1605	0.2098	N/A
StegaNeRF [6]	27.72	0.8340	0.1428	0.9730	**100.0**
Noise-NeRF	**27.74**	**0.8353**	**0.1408**	**0.9913**	**100.0**
Standard NeRF [7]	31.13	0.9606	0.0310	N/A	N/A
LSB [24]	31.12	0.9604	0.0310	0.0830	N/A
DeepStega [27]	31.13	0.9606	0.0313	0.2440	N/A
StegaNeRF [6]	30.96	0.9583	0.0290	0.9677	99.72
Noise-NeRF	**31.13**	**0.9606**	**0.0310**	**0.9847**	**100.0**

Fig. 4 shows that Noise-NeRF continuously optimizes noise through iteration. After inputting the noise, the image rendered by NeRF gradually approaches the target image. After 300 iterations, the SSIM of the rendered hidden image and ground truth are both greater than 98%, which can meet the steganography requirements.

As Table. I shows, Noise-NeRF maintains consistent rendering quality with the standard NeRF. This is because NeRF performs standard rendering as long as no noise is input. However, other methods all modify NeRF's model weights to a certain extent, thus damaging the rendering quality. In terms of steganography quality, Noise-NeRF's SSIM on the two data sets got 0.9913 and 0.9847, respectively, proving the SOTA performance of Noise-NeRF on NeRF steganography.

C. Super-resolution Steganography

In this experiment, we tested the steganography ability of Noise-NeRF on super-resolution images. We randomly select images from the super-resolution dataset as targets, each of which has a 2K resolution. Due to the huge number of bits required for steganography, baseline steganography algorithms

TABLE II: Noise-NeRF on Super-resolution datasets. The results are the average of NeRF-Synthetic and LLFF scenes.

Scene	Dataset	NeRF Rendering			Embed Recovery	
		PSNR	SSIM	LPIPS	PSNR	SSIM
Synthetic	DIV2K	27.74	0.8353	0.1408	48.62	0.9889
	OST				46.58	0.9748
	FFHQ				48.75	0.9889
	CelebA-HQ				46.80	0.9775
LLFF	DIV2K	31.13	0.9606	0.0310	47.90	0.9814
	OST				44.91	0.9704
	FFHQ				47.59	0.9807
	CelebA-HQ				44.77	0.9799

would cause tremendous damage to NeRF-rendered images. The visualization results of the experiment are shown in Fig. 5. We clip the super-resolution image into multiple sub-images and randomly select different viewpoints of the NeRF model. We align different sub-images to different viewpoints and stitch them together to obtain the final result. As shown in Table. II, in different NeRF scenes and different super-resolution datasets, Noise-NeRF achieves a 100% success rate in NeRF steganography, with the steganographic images achieving a similarity of more than 97%. Please refer to Fig. 7 and Fig. 8 for more details on the qualitative results. It proves the superiority of Noise-NeRF on super-resolution image steganography.

D. Ablation Study

We conduct the ablation study by removing various components of Noise-NeRF as shown in Table III to verify the effectiveness of each part. In the experiment we set the number of iterations to 300. As shown in Fig. 6, we take the standard NeRF rendering image and steganographic target as a reference. From Fig. 6 and Table III, we observed that some pixels were completely blank in the output image without Adaptive Pixel Selection. This is because each pixel is different and has a different target pixel, thus requiring different iterations and batch size settings. Our Adaptive Pixel Selection strategy can handle this situation well by selecting pixels in a targeted manner. Removing the Pixel Perturbation Strategy resulted in some pixel noise in the output image. This is because the huge neural network depth of NeRF requires many iterations of backpropagation to update the input noise and slowly gradually converge to the steganographic object. The Pixel Perturbation Strategy increases the difference between the output image and the original image in the early stage, thus accelerating the noise's deviation from the original prediction of NeRF.

TABLE III: Ablation study of Noise-NeRF.

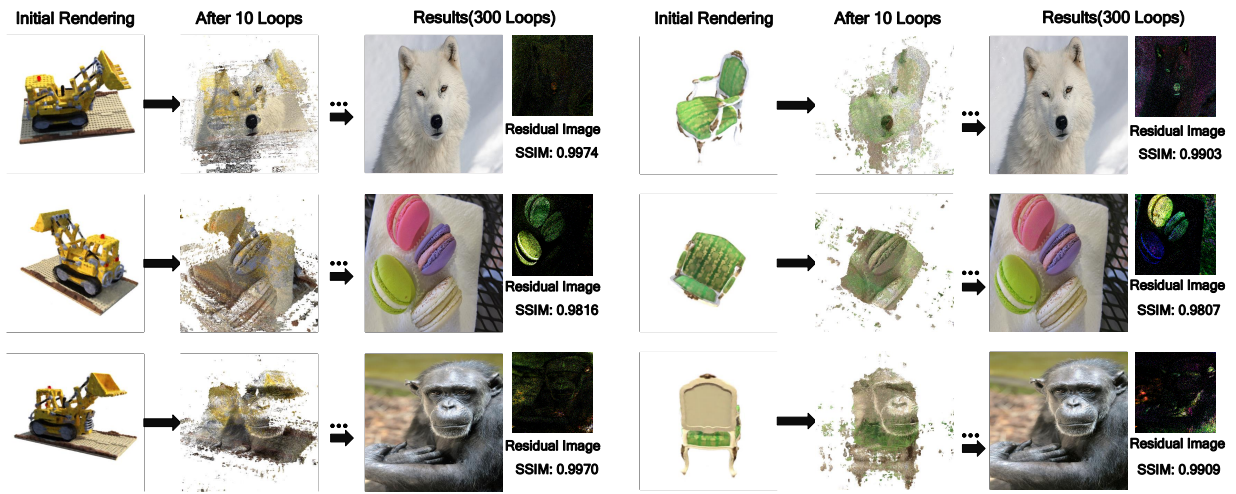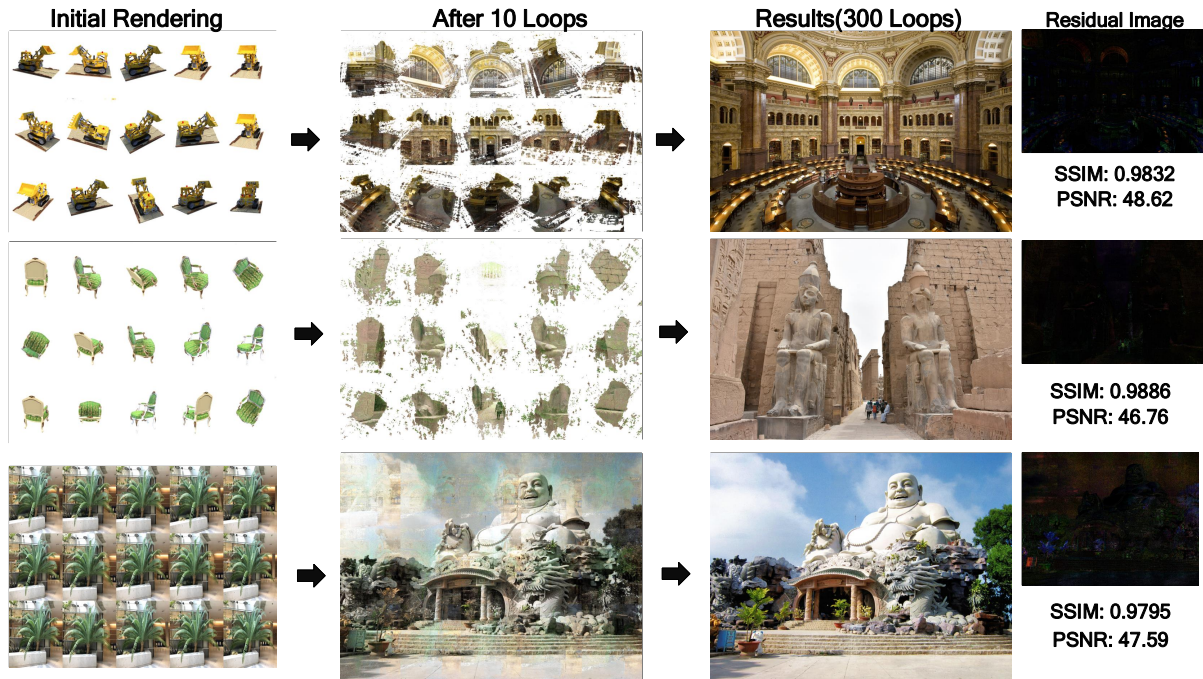| Method	50 Loops		200 Loops		Results(300 Loops)	
	SSIM	Total Loss	SSIM	Total Loss	SSIM	Total Loss
No strategy	0.51	3143.79	0.62	2526.70	0.69	761.63
No Adaptive Pixel Selection	0.44	976.76	0.49	211.35	0.59	83.08
No Pixel Perturbation	0.69	83.67	0.76	66.15	0.82	26.40
Noise-NeRF (complete version)	**0.71**	**74.33**	**0.88**	**13.24**	**0.98**	**0.55**

Fig. 4: Noise-NeRF on multiple scenes.

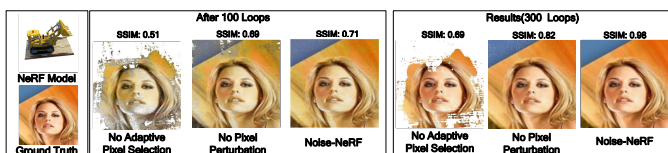Fig. 5: Noise-NeRF on super-resolution images.

Fig. 6: Ablation study of Noise-NeRF.

V. CONCLUSION

In this paper, we propose a NeRF steganography method based on trainable noise, Noise-NeRF, to address challenges faced by NeRF steganography, namely low steganographic quality, model weight damage, and limited steganographic information. We use iterative backpropagation to update the input noise. We propose Adaptive Pixel Selection Strategy and Pixel Perturbation Strategy to improve steganography quality and efficiency. Experimental results prove the superiority of Noise-NeRF over existing baselines in both steganography quality and rendering quality, as well as effectiveness in super-resolution image steganography.

| Initial Rendering | After 10 Loops | Results(300 Loops) | Residual Image |

SSIM: 0.9834
PSNR: 48.24

SSIM: 0.9868
PSNR: 46.57

SSIM: 0.9725
PSNR: 47.53

SSIM: 0.9821
PSNR: 48.45
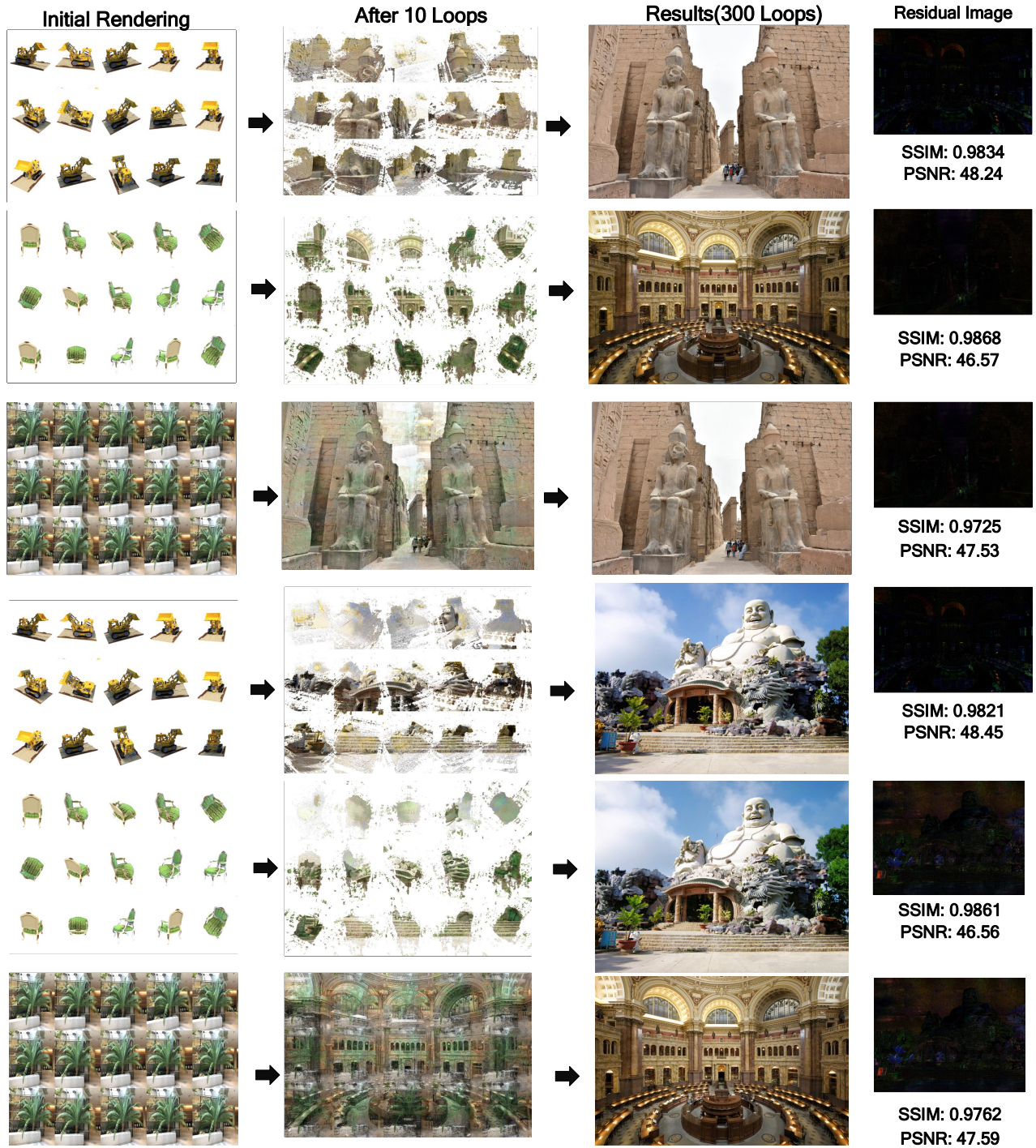
SSIM: 0.9861
PSNR: 46.56

SSIM: 0.9762
PSNR: 47.59

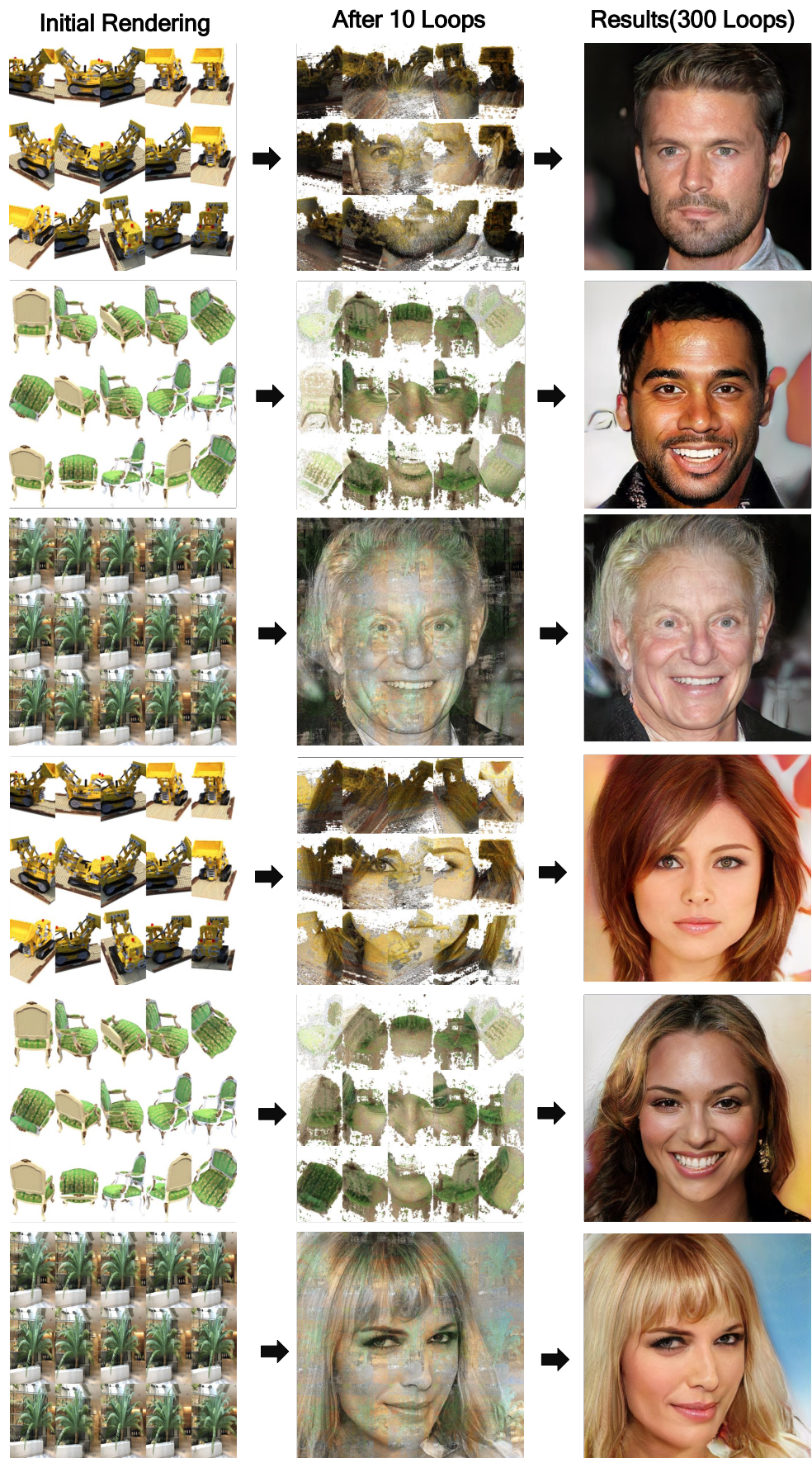Fig. 7: Qualitative results of Noise-NeRF on Super-resolution scenes results.

Fig. 8: More qualitative results of Noise-NeRF on multiple scenes results.

REFERENCES

[1] Matthew Tancik, Ethan Weber, Evonne Ng, Ruilong Li, Brent Yi, Terrance Wang, Alexander Kristoffersen, Jake Austin, Kamyar Salahi, Abhik Ahuja, et al., "Nerfstudio: A modular framework for neural radiance field development," in *ACM SIGGRAPH 2023 Conference Proceedings*, 2023, pp. 1–12.

[2] Jonathan T Barron, Ben Mildenhall, Dor Verbin, Pratul P Srinivasan, and Peter Hedman, "Mip-nerf 360: Unbounded anti-aliased neural radiance fields," in *Proceedings of the IEEE/CVF Conference on Computer Vision and Pattern Recognition*, 2022, pp. 5470–5479.

[3] Deborah Levy, Amit Peleg, Naama Pearl, Dan Rosenbaum, Derya Akkaynak, Simon Korman, and Tali Treibitz, "Seathru-nerf: Neural radiance fields in scattering media," in *Proceedings of the IEEE/CVF Conference on Computer Vision and Pattern Recognition*, 2023, pp. 56–65.

[4] András Horváth and Csaba M Józsa, "Targeted adversarial attacks on generalizable neural radiance fields," in *Proceedings of the IEEE/CVF International Conference on Computer Vision*, 2023, pp. 3718–3727.

[5] Ziyuan Luo, Qing Guo, Ka Chun Cheung, Simon See, and Renjie Wan, "Copyrnerf: Protecting the copyright of neural radiance fields," in *Proceedings of the IEEE/CVF International Conference on Computer Vision*, 2023, pp. 22401–22411.

[6] Chenxin Li, Brandon Y Feng, Zhiwen Fan, Panwang Pan, and Zhangyang Wang, "Steganerf: Embedding invisible information within neural radiance fields," in *Proceedings of the IEEE/CVF International Conference on Computer Vision*, 2023, pp. 441–453.

[7] Ben Mildenhall, Pratul P Srinivasan, Matthew Tancik, Jonathan T Barron, Ravi Ramamoorthi, and Ren Ng, "Nerf: Representing scenes as neural radiance fields for view synthesis," *Communications of the ACM*, vol. 65, pp. 99–106, 2021.

[8] Anpei Chen, Zexiang Xu, Andreas Geiger, Jingyi Yu, and Hao Su, "Tensorf: Tensorial radiance fields," in *Proceedings of the European Conference on Computer Vision (ECCV)*, 2022.

[9] Sara Fridovich-Keil, Alex Yu, Matthew Tancik, Qinhong Chen, Benjamin Recht, and Angjoo Kanazawa, "Plenoxels: Radiance fields without neural networks," in *Proceedings of the IEEE/CVF Conference on Computer Vision and Pattern Recognition*, 2022, pp. 5501–5510.

[10] Thomas Müller, Alex Evans, Christoph Schied, and Alexander Keller, "Instant neural graphics primitives with a multiresolution hash encoding," *ACM Transactions on Graphics (ToG)*, vol. 41, pp. 1–15, 2022.

[11] Chong Bao, Yinda Zhang, Bangbang Yang, Tianxing Fan, Zesong Yang, Hujun Bao, Guofeng Zhang, and Zhaopeng Cui, "Sine: Semantic-driven image-based nerf editing with prior-guided editing field," in *Proceedings of the IEEE/CVF Conference on Computer Vision and Pattern Recognition*, 2023, pp. 20919–20929.

[12] Fangneng Zhan, Lingjie Liu, Adam Kortylewski, and Christian Theobalt, "General neural gauge fields," in *Proceedings of the International Conference on Learning Representations (ICLR)*, 2023.

[13] Junha Hyung, Sungwon Hwang, Daejin Kim, Hyunji Lee, and Jaegul Choo, "Local 3d editing via 3d distillation of clip knowledge," in *Proceedings of the IEEE/CVF Conference on Computer Vision and Pattern Recognition*, 2023, pp. 12674–12684.

[14] Alex Yu, Vickie Ye, Matthew Tancik, and Angjoo Kanazawa, "pixelnerf: Neural radiance fields from one or few images," in *Proceedings of the IEEE/CVF Conference on Computer Vision and Pattern Recognition*, 2021, pp. 4578–4587.

[15] Qianqian Wang, Zhicheng Wang, Kyle Genova, Pratul P Srinivasan, Howard Zhou, Jonathan T Barron, Ricardo Martin-Brualla, Noah Snavely, and Thomas Funkhouser, "Ibrnet: Learning multi-view image-based rendering," in *Proceedings of the IEEE/CVF Conference on Computer Vision and Pattern Recognition*, 2021, pp. 4690–4699.

[16] Tengfei Wang, Bo Zhang, Ting Zhang, Shuyang Gu, Jianmin Bao, Tadas Baltrusaitis, Jingjing Shen, Dong Chen, Fang Wen, Qifeng Chen, et al., "Rodin: A generative model for sculpting 3d digital avatars using diffusion," in *Proceedings of the IEEE/CVF Conference on Computer Vision and Pattern Recognition*, 2023, pp. 4563–4573.

[17] Muhammad Zubair Irshad, Sergey Zakharov, Katherine Liu, Vitor Guizilini, Thomas Kollar, Adrien Gaidon, Zsolt Kira, and Rares Ambrus, "Neo 360: Neural fields for sparse view synthesis of outdoor scenes," in *Proceedings of the IEEE/CVF International Conference on Computer Vision*, 2023, pp. 9187–9198.

[18] Zhenxing Mi and Dan Xu, "Switch-nerf: Learning scene decomposition with mixture of experts for large-scale neural radiance fields," in *Proceedings of the International Conference on Learning Representations (ICLR)*, 2023.

[19] Matthew Tancik, Vincent Casser, Xinchen Yan, Sabeek Pradhan, Ben Mildenhall, Pratul P Srinivasan, Jonathan T Barron, and Henrik Kretzschmar, "Block-nerf: Scalable large scene neural view synthesis," in *Proceedings of the IEEE/CVF Conference on Computer Vision and Pattern Recognition*, 2022, pp. 8248–8258.

[20] ," https://lumalabs.ai/.

[21] Lisa M Marvel, Charles G Boncelet, and Charles T Retter, "Spread spectrum image steganography," *IEEE Transactions on image processing*, pp. 1075–1083, 1999.

[22] Tao Zhang and Xijian Ping, "Reliable detection of lsb steganography based on the difference image histogram," in *Proceedings of IEEE International Conference on Acoustics, Speech, and Signal Processing, 2003.(ICASSP'03).*, 2003, pp. III–545.

[23] Weiqi Luo, Fangjun Huang, and Jiwu Huang, "Edge adaptive image steganography based on lsb matching revisited," *IEEE Transactions on information forensics and security*, pp. 201–214, 2010.

[24] Supriadi Rustad, Abdul Syukur, Pulung Nurtantio Andono, et al., "Inverted lsb image steganography using adaptive pattern to improve imperceptibility," *Journal of King Saud University-Computer and Information Sciences*, pp. 3559–3568, 2022.

[25] Jiren Zhu, Russell Kaplan, Justin Johnson, and Li Fei-Fei, "Hidden: Hiding data with deep networks," in *Proceedings of the European Conference on computer vision (ECCV)*, 2018, pp. 657–672.

[26] Shumeet Baluja, "Hiding images in plain sight: Deep steganography," *Advances in neural information processing systems*, vol. 30, 2017.

[27] Baluja, "Hiding images within images," *IEEE Transactions on Pattern Analysis and machine intelligence*, pp. 1685–1697, 2019.

[28] Gernot Riegler, Ali Osman Ulusoy, and Andreas Geiger, "Octnet: Learning deep 3d representations at high resolutions," in *Proceedings of the IEEE conference on computer vision and pattern recognition*, 2017, pp. 3577–3586.

[29] Emil Praun, Hugues Hoppe, and Adam Finkelstein, "Robust mesh watermarking," in *Proceedings of the 26th annual conference on Computer graphics and interactive techniques*, 1999, pp. 49–56.

[30] Jiahao Zhu, Yushu Zhang, Xinpeng Zhang, and Xiaochun Cao, "Gaussian model for 3d mesh steganography," *IEEE Signal Processing Letters*, vol. 28, pp. 1729–1733, 2021.

[31] Yue Wu, Guotao Meng, and Qifeng Chen, "Embedding novel views in a single jpeg image," in *Proceedings of the IEEE/CVF International Conference on Computer Vision*, 2021, pp. 14519–14527.

[32] Tianhang Zheng, Changyou Chen, and Kui Ren, "Distributionally adversarial attack," in *Proceedings of the AAAI Conference on Artificial Intelligence*, 2019, pp. 2253–2260.

[33] Aleksander Madry, Aleksandar Makelov, Ludwig Schmidt, Dimitris Tsipras, and Adrian Vladu, "Towards deep learning models resistant to adversarial attacks," *arXiv preprint arXiv:1706.06083*, 2017.

[34] Nicholas Carlini and David Wagner, "Towards evaluating the robustness of neural networks," in *2017 IEEE symposium on security and privacy (sp)*, 2017, pp. 39–57.

[35] Ashish Vaswani, Noam Shazeer, Niki Parmar, Jakob Uszkoreit, Llion Jones, Aidan N Gomez, Łukasz Kaiser, and Illia Polosukhin, "Attention is all you need," *Advances in neural information processing systems*, vol. 30, 2017.

[36] Qian Wang, Baolin Zheng, Qi Li, Chao Shen, and Zhongjie Ba, "Towards query-efficient adversarial attacks against automatic speech recognition systems," *IEEE Transactions on Information Forensics and Security*, pp. 896–908, 2020.

[37] Ben Mildenhall, Pratul P Srinivasan, Rodrigo Ortiz-Cayon, Nima Khademi Kalantari, Ravi Ramamoorthi, Ren Ng, and Abhishek Kar, "Local light field fusion: Practical view synthesis with prescriptive sampling guidelines," *ACM Transactions on Graphics (TOG)*, pp. 1–14, 2019.

[38] Jia Deng, Wei Dong, Richard Socher, Li-Jia Li, Kai Li, and Li Fei-Fei, "Imagenet: A large-scale hierarchical image database," in *2009 IEEE conference on computer vision and pattern recognition*. Ieee, 2009, pp. 248–255.

[39] Eirikur Agustsson and Radu Timofte, "Ntire 2017 challenge on single image super-resolution: Dataset and study," in *Proceedings of the IEEE conference on computer vision and pattern recognition workshops*, 2017, pp. 126–135.

[40] Xintao Wang, Ke Yu, Chao Dong, and Chen Change Loy, "Recovering realistic texture in image super-resolution by deep spatial feature transform," in *Proceedings of the IEEE conference on computer vision and pattern recognition*, 2018, pp. 606–615.

[41] Tero Karras, Samuli Laine, and Timo Aila, "A style-based generator architecture for generative adversarial networks," in *Proceedings of the IEEE/CVF conference on computer vision and pattern recognition*, 2019, pp. 4401–4410.

[42] Tero Karras, Timo Aila, Samuli Laine, and Jaakko Lehtinen, "Progressive growing of gans for improved quality, stability, and variation," *arXiv preprint arXiv:1710.10196*, 2017.

[43] Jessica Fridrich, Miroslav Goljan, and Rui Du, "Detecting lsb steganography in color, and gray-scale images," *IEEE multimedia*, pp. 22–28, 2001.